Cd-Substituted Horse Liver Alcohol Dehydrogenase: Catalytic Site Metal Coordination Geometry and Protein Conformation†

L. Hemmingsen,*,‡ R. Bauer,‡ M. J. Bjerrum,§ M. Zeppezauer,|| H. W. Adolph,|| G. Formicka,|| and E. Cedergren-Zeppezauer⊥

Department of Mathematics and Physics and Department of Chemistry, The Royal Veterinary and Agricultural University, Thorvaldsensvej 40, DK-1871 Frederiksberg C, Denmark, Department of Biochemistry, Universität des Saarlandes, Saarbrücken, D-66041, Germany, and Department of Structural Chemistry, Arrhenius Laboratories for Natural Sciences, Stockholm University, S-10691 Stockholm, Sweden

Received October 20, 1994⊗

ABSTRACT: The coordination geometry of the catalytic site in Cd-substituted horse liver alcohol dehydrogenase (LADH) has been investigated as a function of pH using the method of perturbed angular correlation of γ-rays (PAC). LADH in solution fully loaded with cadmium, including radioactive ^{111m}Cd in the catalytic site [$Cd_2(^{111m}Cd)Cd_2$LADH], was studied over the pH range 7.9−11.5. Analysis of the PAC spectra showed the ionization of a group with a pK_a of 11. This pK_a value is about 2 pH units higher than that of native zinc-containing LADH. A pK_a of 9.6 was found for the binary complex of $Cd_2(^{111m}Cd)Cd_2$LADH with NAD^+. This value is also about 2 pH units higher than that of the binary complex of native zinc-containing enzyme and NAD^+. No pH dependency was detected for the binary complex of $Cd_2(^{111m}Cd)Cd_2$LADH with NADH within the pH range measured (pH 8.3−11.5). Assuming that metal-coordinated water is the ionizing group [Kvassman, J., & Pettersson, G. (1979) *Eur. J. Biochem. 100,* 115−123], we conclude that the larger ionic radius of Cd(II) relative to Zn(II) in the catalytic site causes the elevated pK_a values of metal-bound water. Interpretation of nuclear quadrupole interaction (NQI) parameters derived from PAC spectra is based on the use of the angular overlap model, using the coordinates for the catalytic zinc site from the 1.8 Å resolution crystal structure of the ternary complex between LADH, NADH, and dimethyl sulfoxide as a model. Within the limits of uncertainty of the X-ray data, good agreement is obtained between the calculated and measured NQI values for LADH at low pH and for the binary complex of LADH with NADH. However, the high-pH form of LADH and both the low- and high-pH forms of the binary complex with NAD^+ do not agree with this coordination geometry. In these cases we could only achieve agreement between data and model if a local conformational change involving the metal ligand Cys174 was introduced, decreasing the S−Cd−S angle by approximately 20°. Such a local change in conformation might be triggered by the presence of a negatively charged solvent metal ligand causing electrostatic repulsion. The catalytic site is flexible in $Cd_2(^{111m}Cd)Cd_2$LADH, but rigid in coenzyme complexes. The binary complex between NADH and LADH in solution exists in two molecular populations having different coordination geometries. This is manifested as two separate, sharply distinguished NQIs, whereas for the ternary complex between dimethyl sulfoxide, NADH, and LADH only one form is detected.

The detailed description of the electronic and ligand rearrangements at the catalytic site of horse liver alcohol dehydrogenase (LADH)[1] during catalysis is an issue upon which there is as yet no general consensus. The association and dissociation rate constants of NAD^+ and NADH show pH dependencies that are reflected in at least three different pK_a values. The pK_a of 9.2 found for the association rate constants of NAD^+ and NADH to the enzyme, the pK_a of 7.6 for the dissociation rate constant of NAD^+, and the pK_a of 11.2 for the dissociation rate constant of NADH have been explained by the ionization of metal ion-bound water in the free enzyme (pK_a = 9.2), the enzyme NAD^+ complex (pK_a = 7.6), and the enzyme−NADH complex (pK_a = 11.2), respectively (Kvassman & Pettersson, 1979; Andersson et al., 1981). In a high-pH study (Kvassman & Pettersson, 1987), an additional pK_a of 10.4 was suggested to be due to the ionization of Lys228, which is involved in coenzyme binding. Other functional groups near the catalytic site have also been proposed to be responsible for these pH dependencies (Chandrasekhar & Plapp, 1988). The state of ioniza-

† Supported by the Danish Research Council for Natural Sciences and the Deutsche Forschungsgemeinschaft, Schwerpunktprogram Bioanorganische Chemie.

* Author to whom correspondence should be addressed; Phone 4535282307, Fax 4535282350.

‡ Department of Mathematics and Physics, The Royal Veterinary and Agricultural University.

§ Department of Chemistry, The Royal Veterinary and Agricultural University.

|| Universität des Saarlandes.

⊥ Stockholm University.

⊗ Abstract published in *Advance ACS Abstracts,* May 1, 1995.

[1] Abbreviations: PAC, perturbed angular correlation; LADH, horse liver alcohol dehydrogenase (EC 1.1.1.1); $M1_2M2_2$LADH, LADH with metal ion M1 in the catalytic site and metal ion M2 in the noncatalytic site; H_4Cd_2LADH, LADH without metal in the catalytic site and with cadmium in the noncatalytic site; $Cd_2(^{111m}Cd)Cd_2$LADH, LADH fully substituted with cadmium, including radioactive ^{111m}Cd in the catalytic site and cadmium in the noncatalytic site; AOM, angular overlap model; NQI, nuclear quadrupole interaction; EFG, electric field gradient; DMSO, dimethyl sulfoxide; TFE, trifluoroethanol.

0006-2960/95/0434-7145$09.00/0

tion of metal-bound water is closely related to suggestions concerning the mechanisms of proton release from the alcohol substrate. Information about changes in the ligand sphere during catalysis has been obtained by using absorption spectroscopy on catalytic site cobalt-substituted LADH (Sartorius et al., 1987), utilizing the substrate chromophore 4-(*N*,*N*-dimethylamino)cinnamaldehyde (Dunn et al., 1982), as well as NMR measurements on catalytic site ^{113}Cd-substituted LADH (Bobsein & Myers, 1981). Crystal structures of the free enzyme and several ternary complexes provide evidence for changes in protein conformation during the catalytic cycle. The free enzyme is crystallized in an open structure, giving orthorhombic crystals (Eklund et al., 1976), and most ternary complexes are crystallized in a closed conformation, giving triclinic or monoclinic crystals (Eklund et al., 1981; Cedergren-Zeppezauer et al., 1982; Cedergren-Zeppezauer, 1986; Al-Karadaghi et al., 1994) and showing that the enzyme conformation depends on the binding of coenzyme and substrate. Within the uncertainties in atomic position, the catalytic site is left unchanged by these conformational changes (S. Al-Karadaghi, unpublished data). No three-dimensional structure is known that describes the binary NAD^+ complex with LADH, although a structure with NAD^+ and pentafluorobenzyl alcohol exists (Ramaswamy et al., 1994).

We report here a detailed solution study of the NQI as a function of pH for cadmium-labeled LADH and its binary complexes with NADH and NAD^+ in the pH range 7.0–11.5. This is possible due to a new PAC spectrometer (Butz et al., 1989) that gives more than 10 times higher counting statistics, as well as improved time resolution compared to that obtained from previously used PAC spectrometers.

PAC Theory. The PAC method gives information about the types and positions of ligands and is very sensitive to changes in the first coordination sphere, where the movement of a ligand by just a few degrees is detectable. A brief introduction to PAC theory is given here, while a more detailed discussion may be found in Frauenfelder and Steffen (1965). The application of PAC to studies of metalloproteins is described in Bauer (1985). PAC measurements require an isotope that decays by emitting two successive γ-rays, between which there will be an angular correlation in space, e.g., ^{111m}Cd in this study. Since the intermediate energy level decays with a certain lifetime τ, the probability of detecting γ_2 as a function of time after the emission of γ_1 is proportional to the exponential $\exp(-t/\tau)$. The angular correlation is perturbed due to the interaction of the nucleus with its surroundings while it is in the intermediate energy level. Since no external magnetic field is applied, the only important contribution to the perturbation is the interaction between the nuclear quadrupole moment of the isotope and the electric field gradient (EFG) from surrounding charges. Only two parameters are needed to describe the EFG in a randomly oriented ensemble of identical molecules in solution, namely, the numerically largest element in the diagonalized EFG tensor, V_{zz}, and the asymmetry parameter $\eta = |V_{yy} - V_{xx}|/|V_{zz}|$. η is zero for an axial symmetric EFG and is always between zero and unity in value. When using ^{111m}Cd, the effect of this perturbation can be described by the function

$$P(\theta,t) \propto \exp(-t/\tau)\left[1 + A_2\left(\frac{3}{2}\cos^2(\theta) - \frac{1}{2}\right)G_2(t)\right] \quad (1)$$

where $P(\theta,t)$ is the probability density of detecting γ_2 at an angle θ with respect to the direction of γ_1 at time t after the detection of γ_1, and A_2 is a constant depending on the nuclear spins involved. The factor $G_2(t)$ describes the perturbation due to the EFG. Experimentally, $G_2(t)$ can be obtained by writing the following expression using eq 1:

$$A_2G_2(t) = 2\frac{W(180°,t) - W(90°,t)}{W(180°,t) + 2W(90°,t)} \quad (2)$$

where $W(180°,t)$ and $W(90°,t)$ are the coincidence counts in 180° and 90°, respectively, at time t.

For ^{111m}Cd, the intermediate level has a spin equal to 5/2, and the EFG splits the energy into three levels. Among these three levels, three energy differences exist. Each energy difference, ΔE_i, gives rise to an oscillation in $G_2(t)$ with a frequency $\omega_i = 2\pi\Delta E_i/h$, where h is Planck's constant. This means that

$$G_2(t) = a_0 + a_1\cos(\omega_1 t) + a_2\cos(\omega_2 t) + a_3\cos(\omega_3 t) \quad (3)$$

where each frequency is proportional to $|V_{zz}|$ with a proportionality constant depending on η. The four amplitudes, a_0, ..., a_3, also depend on η. The Fourier transformation of the function $A_2G_2(t)$ thus should consist of three peaks for each coordination geometry in which ^{111m}Cd exists. In such a case, we can write

$$G_2(t) = \sum_{j=1}^{n} f_j G_2^j(t) \quad (4)$$

where j refers to the jth EFG present at a relative fraction f_j. In the data analysis of PAC spectra, it is also necessary to include rotational diffusion and frequency distributions in $G_2(t)$.

The Brownian motion of the molecules implies that the EFG at the nucleus of ^{111m}Cd reorients. The reorientation is characterized by τ_r, the rotational diffusion time, and its effect on $G_2(t)$ can be found in Danielsen et al. (1991). Small structural variations in the coordination geometry for ^{111m}Cd in the ensemble of molecules lead to a distribution of EFG values. This can be described by a Gaussian distribution of EFGs with a relative width of δ. This frequency distribution is a measure of the rigidity of the metal site.

MATERIALS AND METHODS

The chemicals were reagent grade or analytical grade when required. NAD^+ and NADH, both 99% pure, were purchased from Sigma and used without further purification. The starting material for a PAC experiment, H_4Cd_2LADH (an enzyme depleted of metal in the active site with Cd_2 in the noncatalytic site), was prepared by a multistep procedure. Native Zn_2Zn_2LADH (EE isoenzyme) was dialyzed at pH 5.5 against 0.1 M acetate buffer containing 10 μM cadmium acetate, similar to that described by Sytkowsky and Vallee (1979). A nearly quantitative exchange of zinc for cadmium in the noncatalytic site was achieved. This enzyme product, Zn_2Cd_2LADH, was crystallized in *tert*-butyl alcohol, and zinc was removed from the catalytic site according to Maret et al. (1979). The catalytic site metal-depleted protein (in 0.16 M Na_2SO_4) was frozen in liquid nitrogen and stored at −80 °C. All water was distilled twice, and adjustment of pH was done by using either NaOH or sulfuric acid in order to avoid

Cl^-. All glassware was washed in aqua regia, and all water was passed through a diethylenetriaminepentaacetate-coupled gel (height = 3 cm, diameter = 1 cm) (Bauer et al., 1991b) in order to lower the contamination of metals to less than 0.1 μM.

^{111m}Cd Production. ^{111m}Cd is produced by irradiating ^{108}Pd on a small graphite block with 21 MeV α-particles for 1.5 h in a beam of about 30 μA. The procedure for ^{111m}Cd production was slightly different from that described earlier (Bauer et al., 1991c). ^{108}Pd (27−28 mg) enriched to 99.2% was dissolved in 0.3 mL of 47% HBr and 0.1 mL of concentrated HNO_3, evaporated to dryness, redissolved in 0.3 mL of 47% HBr and 2 mL of concentrated NH_4, and left overnight. Before electrolysis, the surface of the graphite target was roughened, washed with 0.2 mL of acetone and with 0.2 mL of aqua regia, and put in an oven at 100 °C for 1 h. The electrolysis was done in three steps, which empirically has turned out to give the best results: (1) The solution was split in two. The first half was electrolyzed for 5 min at 1.7 V, giving a current of approximately 5 mA, to obtain a smooth first layer of ^{108}Pd. (2) Electrolysis was continued for 60 min at 1.8 V, giving a current typically decreasing from 12 to 4 mA. (3) The second half of the solution was electrolyzed for 70 min at 1.8 V, giving a current decrease from about 10 to 3 mA. Typically, 14 mg of ^{108}Pd was deposited, in a circular spot with a diameter of 1 cm, on the graphite target. The electrolysis was done with the target as cathode and a Pt wire as anode. The total ^{111m}Cd activity immediately after irradiation ranged between 200 and 900 MBq (less than 10 pmol of cadmium). The ^{111m}Cd was extracted from the target by washing it in 400 μL of aqua regia, giving a yield of 60−90% of the total activity, followed by evaporation to dryness, redissolution of the active material in 400 μL of concentrated HCl, evaporation to dryness, and addition of 500 μL of water. Palladium is primarily in the form $[PdCl_4]^{2-}$, due to its strong affinity for Cl^-, while cadmium is found primarily with two bound Cl^-, making separation of the two metals possible by using an anion exchange column. The solution was filtered with a 0.22 μm filter and separated on an anion exchange column (IRA-420C), using water as eluent. The fractions containing the activity were pooled and evaporated to about 85 μL.

Reconstitution of the Catalytic Site in LADH with Cd. The reconstitution of H_4Cd_2LADH was typically carried out by mixing all $^{111m}Cd^{2+}$ with 45 μL of 0.5 mM cadmium acetate and 100 μL of 0.5 M Tris−SO_4 (pH 8.5). This solution was then added to 20 μL of 49 mg/mL H_4Cd_2LADH in 0.16 M $NaSO_4$. The concentrations after mixing were 2−10 nM $^{111m}Cd^{2+}$, 90 μM cadmium acetate, 50 μM LADH, 13 mM Na_2SO_4, and 200 mM Tris−SO_4. Since there are two catalytic sites (LADH is a dimer), this gives 90% reconstitution of the catalytic metal site, if all of the cadmium binds. The solution was left for 10 min for Cd^{2+} to coordinate. Free cadmium was separated from enzyme-bound cadmium by gel filtration on a Sephadex G-25 column (height = 18 cm, diameter = 1 cm), with 75 mM Tris−SO_4 buffer as eluent. The pH used was between 7.0 and 8.5 and typically gave a protein peak containing 70% of the radioactive cadmium, leaving a salt fraction of 30% free $^{111m}Cd^{2+}$. This is in good agreement with the 10 min binding time, according to Skjeldal et al. (1982). After this the coenzyme was added. In the last steps, before the PAC experiment, sucrose was added to 55% (w/w) and the pH was adjusted, giving a final sample volume between 400 μL and 2.5 mL. All manipulation before the PAC experiment was performed at room temperature, whereas the PAC experiments were carried out at 4 °C. In selected cases the enzyme activity was tested after the PAC experiment by the method of Dalziel (1957).

pH Measurement. The pH was measured just before the PAC experiment in the sucrose solution at room temperature. All pH values given in this study are referenced to 1 °C in 55% (w/w) sucrose. It was found that there is a linear relation between the pH at 1 °C and that at 25 °C over the pH range 7−10 in a 40 mM Tris/55% (w/w) sucrose solution. The pH values of the PAC measurements were corrected to pH at 1 °C by using the relation pH(1 °C) = 0.926pH(25 °C) + 0.86.

NADH and NAD^+ Binding to the Cadmium Enzyme. Dissociation constants were determined in titration experiments monitoring the decrease in protein fluorescence (excitation 285 nm, emission 330 nm) due to coenzyme coordination. The enzyme used was Cd_2Zn_2LADH, which behaves very similar to the fully Cd^{2+}-substituted enzyme. The enzyme concentration was 0.1 μM in the NADH binding experiments and 0.2 μM when NAD^+ binding was studied. Enzyme was titrated with coenzyme stock solutions 78 μM NADH and 246 μM NAD^+, respectively. The protein fluorescence observed was corrected for inner filter effects. The resulting data sets of typically 10−15 titration steps have been evaluated by using a numerical integration procedure allowing simultaneous fitting of binding constants and the relative fluorescence factors of free enzyme and enzyme−coenzyme complexes. Each determination was performed four times, and data given are the corresponding averages with standard deviations.

PAC Setup. The PAC spectrometer consists of six detectors arranged such that each detector is directed toward one plane of an imaginary cube, in the center of which the sample is positioned. It is a slightly modified version of the "PAC-camera" described by Butz et al. (1989). The modified version has the facility for automatic adjustment of detector−sample distance, making it possible to keep an optimal counting rate until the activity has decayed so much that the sample−detector distance is the smallest possible. The temperature of the sample was controlled by a Peltier element lying about 2 cm below the sample. The temperature of the sample can be set in the range −10 to 40 °C, with an accuracy of ±2 °C. The time resolution of the instrument is 850 ps.

Analysis of PAC Spectra. Six combinations of 180° coincidence spectra and 24 combinations of 90° coincidence spectra were collected. In each coincidence spectrum the background due to accidental coincidences was subtracted. Using a ^{75}Se source as a time calibration standard, the spectra were adjusted in channels such that a specific time delay between the two γ-rays occurs in the same channel in all spectra. The measured $A_2G_2(t)$ was constructed from the 30 coincidence spectra as given in eq 2, where $W(180°,t)$ is the 6th root of the product of the six 180° coincidence spectra and the equivalent for $W(90°,t)$. The theoretical $A_2G_2(t)$ containing five fitting parameters, ω_0, η, δ, A_2, and τ_r, was fitted to the experimental $A_2G_2(t)$ by conventional χ^2 minimization (see eqs 2−4). ω_0 is proportional to the numerically largest element in this diagonalized EFG tensor, V_{zz}:

$$\omega_0 = \frac{6\pi}{20h}|V_{zz}eQ|$$

where Q is the nuclear quadrupole moment and h is Planck's constant. When more than one NQI appears in a PAC spectrum, the relative fractions of the individual NQIs were also determined (see eq 4). A_2, the amplitude of the perturbation, for ^{111m}Cd has a maximum value of 0.18 (Aeppli et al., 1951) but the experimental value normally is significantly lower due to the finite size of the sample and detectors.

AOM Calculations. Given the crystal structure of a cadmium complex, ω_0 and η can be calculated by using the AOM (Bauer et al., 1988). In our use of this semiempirical model, it is assumed that each ligand contributes with an axial symmetric tensor of strength ω_l (l for ligand), with the symmetry axis given by the Cd−ligand bond. For ^{111m}Cd, ω_l, also called the partial nuclear quadrupole interaction parameter, depends only on the ligand. The partial NQIs for all of the ligands considered in this paper, except OH^- and dimethyl sulfoxide (DMSO), have been determined from experiments on crystalline model compounds with known structure (Bauer et al., 1988, 1991a). The total NQI from all of the ligands is calculated by adding the tensor from each ligand and diagonalizing this sum tensor. The experimental ω_0 and η can be compared with those calculated from the crystal structure of a protein complex.

It is necessary to account for the uncertainties in the ligand−metal−ligand angles determined by X-ray crystallography and in the partial NQIs determined by PAC spectroscopy on crystalline model compounds, as well as uncertainty in the ω_0 and η values determined by PAC spectroscopy. We therefore construct the following χ^2 sum:

$$\chi^2 = \frac{(\omega_0^m)^2}{\sigma^2(\omega_0^m)} + \frac{(\eta^m - \eta^f)^2}{\sigma^2(\eta^m)} + \sum_{\text{ligands}} \left[\frac{(\theta_{lig}^m - \theta_{lig}^f)^2}{\sigma^2(\theta_{lig}^m)} + \frac{(\phi_{lig}^m - \phi_{lig}^f)^2}{\sigma^2(\phi_{lig}^m)} + \frac{(\omega_{lig}^m - \omega_{lig}^f)^2}{\sigma^2(\omega_{lig}^m)} \right] \quad (5)$$

where the indices m and f refer to measured and fitted values, respectively, and σ is the standard deviation of the corresponding parameter. θ_{lig} and ϕ_{lig} are the polar angle and the azimuthal angle for the ligand in a coordinate system, respectively, in which one of the metal-coordinating atoms is positioned along the z-axis and another defines the x, z plane. The χ^2 sum in eq 5 is minimized with respect to the variables θ_{lig}^f, ϕ_{lig}^f, and ω_{lig}^f. ω_0^f and η^f are dependent variables, calculated using the AOM, given a set of suggested values for θ_{lig}^f, ϕ_{lig}^f, and ω_{lig}^f. The ligand sphere for the catalytic metal site in LADH, used in the minimization of the χ^2 sum in eq 5, consists of His67, Cys46, Cys174, and a solvent molecule. The crucial point in the minimization procedure is to choose reasonable values for the standard deviations on the angles, the partial NQIs, and ω_0^m and η^m. We have chosen 5° for the angles, except for the solvent ligand for which a greater freedom, namely, 10°, was allowed. The experimental standard deviations of ω_0 and η are 0.3−4 Mrad/s and 0.001−0.05, respectively. It is not to be expected that the AOM can calculate NQI to such an accuracy. In addition, charges outside the first coordination sphere are not included in the AOM calculations. A unit point charge in the second coordination sphere with a distance of 5−6 Å will contribute with a partial NQI of about 10 Mrad/s. Therefore, the standard deviations of ω_0 and η used in the χ^2 minimization were set to 10 Mrad/s and 0.05, respectively. For the same reasons the standard deviations of the partial NQIs were set to 10 Mrad/s.

Table 1: Equilibrium Constants for the Complexes of NADH and NAD^+ to Zn_2Zn_2LADH and Cd_2Zn_2LADH

ligand	enzyme	buffer	pH	T (°C)	K_d (μM)
NADH	Zn_2Zn_2LADH	50 mM TAPS	8.5	25	0.18(±0.02)
		50 mM TES	7.0	25	0.10(±0.02)
	Cd_2Zn_2LADH	50 mM Tris	8.0	25	0.026(±0.004)
		50 mM Tris[a]	8.0	25	0.028(±0.005)
		50 mM Tris	8.0	7	0.024(±0.005)
NAD^+	Zn_2Zn_2LADH	50 mM TAPS	8.5	25	5.7(±0.7)
		50 mM TES	7.0	25	7.0(±1.2)
	Cd_2Zn_2LADH	50 mM Tris	8.0	25	7.2(±0.3)
		50 mM Tris[a]	8.0	25	5.1(±0.2)
		50 mM Tris	8.0	7	7.9(±0.3)

[a] In 52% sucrose.

RESULTS

The binding constants for NADH and NAD^+ to LADH with cadmium in the catalytic site are given in Table 1. Binding of NADH is about 1 order of magnitude stronger for the Cd-substituted enzyme than for the native zinc enzyme. NADH binding is unaffected by the addition of sucrose or lowering of the temperature from 25 to 7 °C. In case of NAD^+ binding to Zn_2Zn_2LADH or Cd_2Zn_2LADH very similar results are obtained. A marginal effect is seen upon the addition of sucrose, but no difference is observed by lowering the temperature.

PAC measurements have been performed on $Cd_2(^{111m}Cd)$-Cd_2LADH as a function of pH for LADH (pH 7.9−11.5), the binary complex between NADH and LADH (pH 8.3−11.5), and the binary complex between NAD^+ and LADH (pH 7.0−11.2). The enzyme apparently is stable for several hours at 1 °C and 55% sucrose at pH 11.5. However, one measurement at pH 12.0 gave a spectrum typical of denatured protein.

It was necessary to include an NQI representing cadmium in the structural site (Andersson et al., 1982). In this study, H_4Cd_2LADH was used in order to have ^{111m}Cd only in the catalytic site. However, when ^{111m}Cd is added to H_4Cd_2-LADH, a fraction of $^{111m}Cd^{2+}$ moves into the structural site due to exchange between the two metal sites. Our experiments indicate that a fraction of typically 10% is bound at the structural site. This migration effect thus is less pronounced for H_4Cd_2LADH than for H_4Zn_2LADH (Andersson et al., 1982). The experimental values of ω_0, δ, η, and τ_r, determined from the measurements on LADH and the binary complexes with NAD^+ and NADH, are presented in Table 2, which also includes the NQI for the ternary complex with NADH and DMSO. Figure 1 shows the Fourier transform of spectra calculated from the parameters given for each NQI in Table 2. The NQI parameters for LADH and for the binary complex between NADH and LADH were obtained by χ^2 fitting to the sum of all obtained spectra for each of the two systems. The two NQIs found for $Cd_2(^{111m}Cd)Cd_2$LADH represent a high-pH form at $\omega_0 = 128$ Mrad/s and a low-pH form at 270 Mrad/s. An NQI with ω_0 equal to 59 Mrad/s arises from $^{111m}Cd^{2+}$ in the structural site of LADH and is found in all systems. The binary complex between LADH and NADH also contains two NQI for the catalytical site with $\omega_0 = 333$ and 326 Mrad/s; however, these two forms are independent of pH. The binary complex

Table 2: Parameters Fitted to PAC Spectra from $Cd_2(^{111m}Cd)Cd_2$LADH Measured in 55% Sucrose at 4 °C in Tris−Sulfate (30−40 mM)

type of complex with LADH[a]	ω_0 (Mrad/s)	η	δ (%)	τ_r (ns)
low-pH form	270 ± 4	0.94 ± 0.05	7.4 ± 0.8	244 ± 24
high-pH form	128 ± 4	0.82 ± 0.02		
NAD^+ low-pH form	178 ± 1	0.79 ± 0.01	2.8 ± 0.4	200
NAD^+ high-pH form	121 ± 1	0.80 ± 0.01		
NADH + DMSO	344 ± 1	0.844 ± 0.002	0.5 ± 0.2	425 ± 110
NADH NQI_1	333 ± 1	0.885 ± 0.004	1.2 ± 0.1	196 ± 19
NADH NQI_2	326 ± 1	0.789 ± 0.006		

[a] The enzyme concentration was between 3.2 and 8.9 μM. The NADH and NAD^+ concentrations were between 4.1 and 6.1 mM, and the concentration of DMSO was 0.1 M. All of the theoretically fitted PAC spectra include a signal with ω_0 at about 59 Mrad/s and η at about 0.9, due to ^{111m}Cd in the structural site (Andersson et al., 1982). NQI_1 determined for the binary NADH complex represents a fraction of 0.4 ± 0.04; NQIs represent a fraction of 0.6. The two NQIs found for the binary NADH complex are included in the χ^2 minimalization of the PAC spectra for the binary NAD^+ complex, with ω_0 and η for the two NQIs for the binary NADH complex (see text). The frequency distribution δ and rotational diffusion time τ_r are assumed equal for the NQIs for the low- and high-pH forms and for the two NQIs observed in the presence of NADH, respectively. The rotational diffusion time τ_r is fixed to 200 ns for the binary complex with NAD^+.

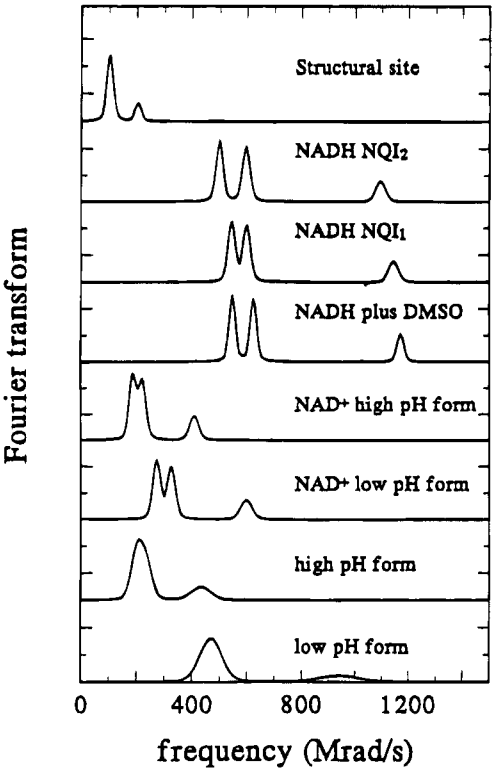

FIGURE 1: Fourier transforms of PAC spectra calculated with NQI parameters for each form as given in Table 2. Note that, because of the large value for the frequency distribution for free LADH (two lowest spectra), it is not possible to separate the two lowest frequency components.

between LADH and NAD^+ contains a high-pH form, with ω_0 equal to 121 Mrad/s and a low-pH form with ω_0 equal to 178 Mrad/s. The spectra were, however, complicated by the presence of NADH. This originates from an extraneous substrate of unknown nature producing NADH during the data collection time. Only spectra for which the fraction of NQIs from the binary complex with NAD^+ is larger than 25% were used (see eq 4). The NQI parameters at low and high pH for the binary NAD^+ complex were determined from

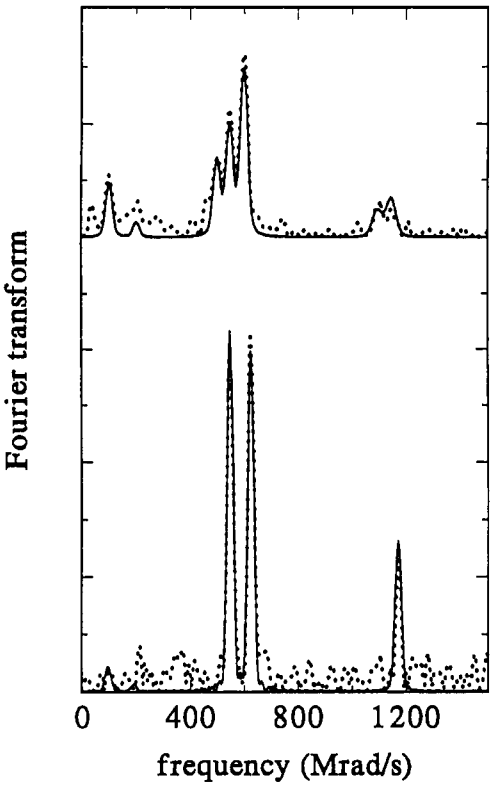

FIGURE 2: Upper panel: Fourier transformation of PAC spectra for the sum of all measurements on the binary complex between $Cd_2(^{111m}Cd)Cd_2$LADH and NADH (pH between 8.3 and 11.5). Lower panel: Fourier transformation of the PAC spectrum for the ternary NADH−DMSO complex at pH 9.1 (Fourier transformation of the PAC spectrum, dotted line; Fourier transformation of the fit to the spectrum, solid line).

the sum of three PAC spectra at low pH and the sum of two PAC spectra at high pH, respectively.

Figure 2 shows the Fourier transform of the sum spectrum for the binary NADH complex compared with the Fourier transform of the PAC spectrum for the ternary complex with NADH and DMSO. In Figure 3, the Fourier transform of the sum spectrum for LADH is shown together with the two sum spectra for the binary complex with NAD^+. For the PAC spectra at different pH values for free LADH and for the binary complex with NAD^+, the relative fractions (f_j in eq 4) of the different NQIs present were determined (the NQI parameters were fixed to the values given in Table 2). The Fourier transform of these fits together with the Fourier transform of the measured data is shown in Figure 4a for free LADH and in Figure 4b for the binary complex with NAD^+. The contribution from the binary NADH complex has been subtracted from the data and the fit shown in Figure 4b. The fraction of the low-pH form as a function of pH is shown in Figure 5a for free LADH and in Figure 5b for the binary NAD^+ complex with LADH. The Fourier transform of PAC spectra from LADH shows a change from high to low ω_0 and a small downward shift in η with increasing pH, with a pK_a of 11.0 ± 0.2 (see Figures 4 and 5). The frequency spread of 7.4% is large and shows up as broad peaks in the Fourier transform (see Figure 3). The measurements on the binary NAD^+ complex with LADH are characterized by having low ω_0 values for both the low- and high-pH forms. The pH dependency can be fitted with a pK_a of 9.6 ± 0.2. The frequency distribution of 2.8% is small relative to that determined for the free enzyme. The measurements on the binary NADH complex (Figure 2 and

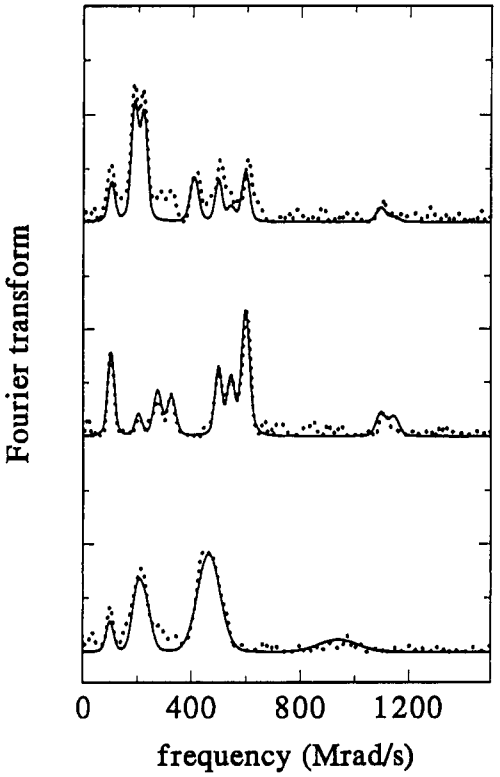

FIGURE 3: Upper panel: Fourier transformation of the sum of two PAC spectra for the NAD^+ complex (pH 10.4 and 11.2). Middle panel: Fourier transformation of the sum of three PAC spectra for the NAD^+ complex (pH 7.0, 8.0, and 8.5). Lower panel: Fourier transformation of the sum PAC spectra for all measurements on the free enzyme. Line types same as for Figure 2.

Table 2) gave two distinct NQIs, both with high ω_0 values, and the parameters are independent of pH in the range 8.3–11.5. The average values for the fraction of the two NQIs are 0.4 and 0.6, respectively. The frequency distribution of 1.2% is low.

Angular Overlap Model Calculations of Nuclear Quadrupole Interactions. Table 3 shows the minimized sum of χ_r^2 calculated from eq 5, using the crystal structure of the ternary complex of Zn_2Zn_2LADH, NADH, and DMSO at 1.8 Å resolution (Al-Karadaghi et al., 1994). If the minimal χ_r^2 is greater than 3, the ligand sphere tested is rejected (5% significance level). Rejection means that ω_0 and η values from the PAC measurements are incompatible with the coordination geometry tested. For the low-pH form for LADH and the two NQIs detected for the binary complex between NADH and LADH, use of an S–Cd–S angle equal to 129° gives an acceptable χ_r^2, whereas for the high-pH form for LADH and both the low- and high-pH forms for the binary NAD^+ complex, the use of this angle cannot give χ_r^2 less than 3. If the Cys174 sulfur is moved toward the Cys46 sulfur, such that this angle is now 107°, acceptable values for χ_r^2 can be obtained for these three cases. It can also be seen from the χ_r^2 values in Table 3 that both NQIs for the binary complex with NADH can be calculated with the X-ray structure geometry and not with the modified structure with the reduced S–Cd–S angle. The choice of 107° as the S–Cd–S angle was made on the basis of analysis of the NQI parameters for the ternary complex with NAD^+ and Cl^- (Bauer et al., 1991a) because the partial NQI parameter for Cl^- is known. In the fit to ω_0 and η of this complex using eq 5, the water ligand was substituted with Cl^- and the S–Cd–S angle was fitted as a free parameter, giving a

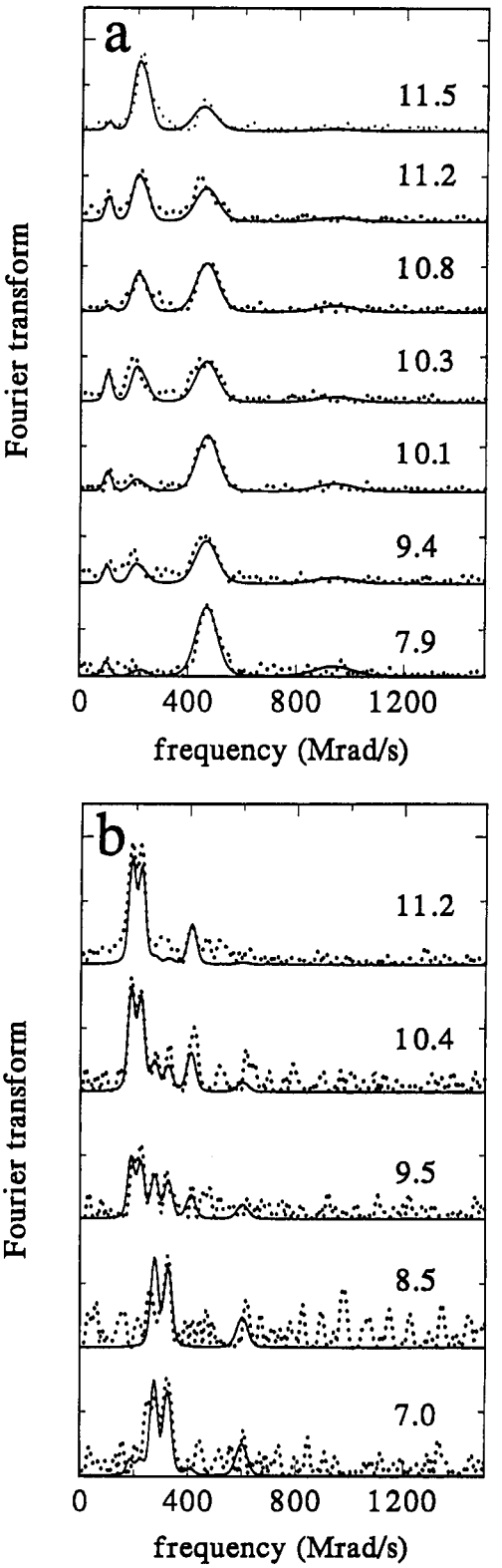

FIGURE 4: Fourier transformations of PAC spectra as a function of pH with the NQI parameters fixed. Only the relative fractions of the different NQIs (see eq 4) and the baseline in the spectrum are fitted. (a) Spectra for different pH values for LADH. (b) Spectra for different pH values for the binary NAD^+,LADH complex. The pH value for each spectrum is indicated at the far right of the spectrum. The contribution from the binary NADH,-LADH complex has been subtracted from the data and the fit shown for the binary NAD^+ complex. The consequences of this is a relative increase in the noise in the Fourier transform of the data. Line types same as for Figure 2.

value of 107°. For the two high-pH forms, χ_r^2 values less than 3 are obtained for S–d–S angles up to 115°, whereas

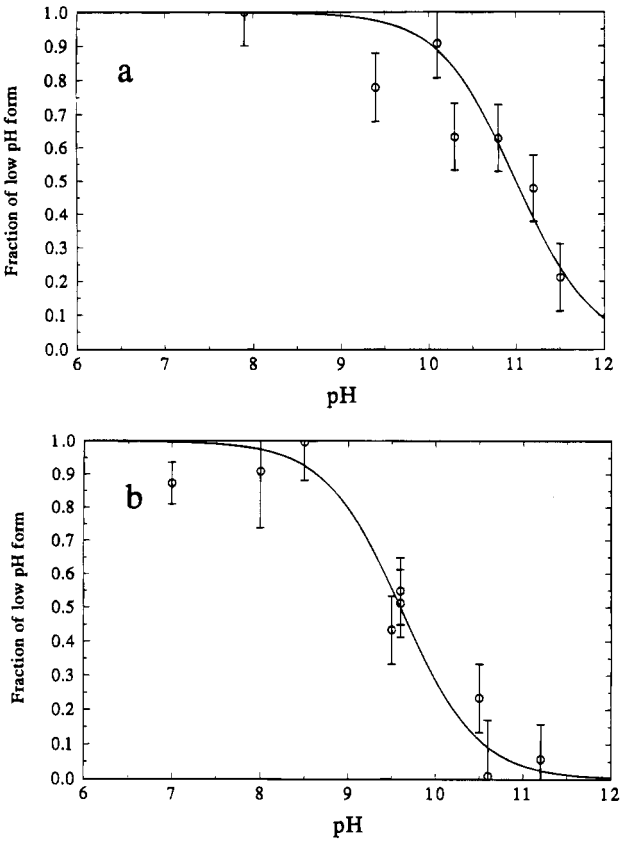

FIGURE 5: Fractions of the low-pH form as a function of pH for free LADH (a) and the binary NAD^+,LADH complex (b). At each pH value, the sum of the fractions for the low- and high-pH forms is normalized to 1.

Table 3: AOM Calculation of NQIs for ^{111m}Cd in $Cd_2(^{111m}Cd)Cd_2LADH$

type of complex with LADH	solvent ligand	χ_r^2 [a] S−Cd−S angle 129°	χ_r^2 [a] S−Cd−S angle 107°
low-pH form	H_2O	0.5	2.2
high-pH form	any	*6.5*	0.9
NAD^+ low-pH form	H_2O	*4.4*	0.2
NAD^+ high-pH form	any	*7.2*	1.0
NADH NQI_1	H_2O	2.3	*5.0*
NADH NQI_2	H_2O	1.4	*4.0*

[a] The χ^2 sum in eq 5 is minimized. The reduced χ_r^2 minima are shown for the S−Cd−S angles equal to 129° and 107°. Values of χ_r^2 larger than 3 (italics, 5% significance level) are considered unacceptable. Any means that the partial NQI ω_l for the solvent ligand was left completely free in the fit.

for the low-pH form with NAD^+, angles up to 120° can be accepted. To show the necessity of a change in the S−Cd−S angle from 130°, we calculated the frequency of ω_0 values for each ligand moved up to 30°, in steps of 5°, from its original position in the Zn_2Zn_2LADH structure with NADH and DMSO. Only the S−Cd−S angle was fixed, first to 130° in agreement with X-ray crystallography and second to 110°. The ω_0 values, for which η is between 0.5 and 1, were added in intervals of 5 Mrad/s. The restriction on η was made because no η value below 0.5 has been observed for LADH. The result shows that, for 130°, no ω_0 values lower than 220 Mrad/s exist (Figure 6).

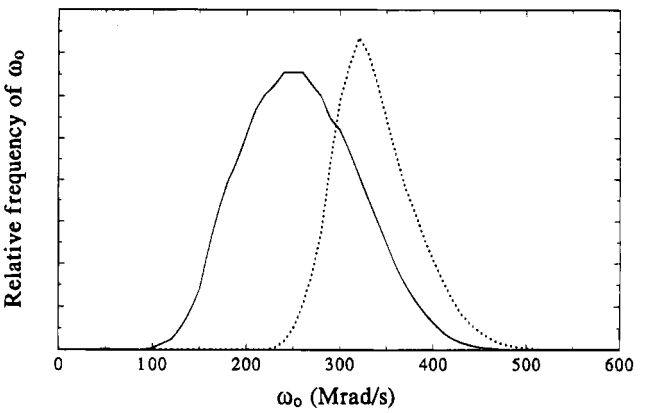

FIGURE 6: Frequency of ω_0 values for NQIs, with η in the interval 0.5−1.0, for two sulfurs from cysteine ligands, one nitrogen from a histidine, and a metal-bound solvent ligand with a partial NQI between 95 and 350 Mrad/s, calculated using the AOM. The result for the S−Cd−S angle fixed to 110° is shown as a solid line, and the result for the S−Cd−S angle fixed to 130° is shown as a dotted line. All other angles were allowed to vary to a maximum of 30° compared to the values found for the X-ray structure of the Zn_2-Zn_2LADH−NADH−DMSO complex (Al-Karadaghi et al., 1994).

DISCUSSION

Local Conformational Changes. The NQIs found for ^{111m}Cd in the catalytic site of $Cd_2(^{111m}Cd)Cd_2LADH$ at low pH and for its NADH complex agree well with the crystal structure of the ternary complex between the native zinc enzyme, NADH, and DMSO. The NQIs for LADH at high pH and for the binary NAD^+,LADH complex at low or high pH cannot have a similar coordination geometry (Table 3). However, these NQIs can be calculated for a coordination geometry where the Cys174 sulfur is moved 22° toward the Cys46 sulfur. That this angular movement is required can be seen in Figure 6. For the S−Cd−S angle fixed to 130°, but allowing a large degree of freedom in angular position for all other angles, no ω_0 value below 220 Mrad/s is possible. This is based on the assumption of four coordination and the validity of the AOM. Five coordination with the fifth ligand in a position opposite to the histidine ligand can, however, also produce low ω_0's. Model building based upon the crystal structure of the ternary NADH,DMSO complex (Al-Karadaghi et al., 1994) shows that the only possibility of five coordination is that of Glu68 (Bauer et al., 1991a). This position has been attempted with the present data by applying the AOM, but such a structure was not able to generate the measured NQI. Furthermore, quantum mechanical calculations consistently do give more unfavorable energies for the five-coordinated catalytic metal site (Ryde, 1994). For these reasons, we disregard five coordination and are left with reduction in the S−Cd−S angle to about 110°. It is noteworthy that quantum mechanical calculations with an OH^- ligand bound to the catalytic site zinc in LADH do predict a value close to 110° for the S−Zn−S angle (Ryde, 1994). Whether or not the reduction in the S−metal−S angle reflects a larger scale conformational change of the enzyme cannot be decided from this work. The low S−Cd−S angle also explains the low ω_0 values obtained previously (Andersson et al., 1981; Bauer et al., 1991a) for the ternary $Cd_2(^{111m}Cd)Zn_2LADH$ complexes with NAD^+ plus Cl^- or TFE^-.

A plausible explanation for the reduction in the S−Cd−S angle is an electrostatic repulsion between the negative charges of the two cysteine sulfurs and a negative charge from a solvent ligand, i.e., OH^- for the high-pH forms for the free enzyme and the NAD^+ complex and Cl^- and TFE^- in ternary complexes with NAD^+. The concept of electrostatic repulsion does not explain the need for the low

S−Cd−S angle for the low-pH form with NAD^+ with water as the solvent ligand. However, in this case the angle only has to be less than 120° (see the Results section). That the electronic configuration is important for an S−metal−S angle was demonstrated recently for zinc complexes (Bochmann et al., 1994).

pH Dependencies. Previous experiments using ^{111m}Cd PAC and ^{113}Cd NMR (Andersson et al., 1982; Bobsein & Myers, 1981) were not able to detect any change in spectral parameters with pH for cadmium in the catalytic site of LADH, except for a slight shift and broadening in a ^{113}Cd NMR spectrum occurring at pH 10.3. From this work it seems that the pH values investigated were not high enough. However, Bobsein and Myers (1981) suggested that line broadening observed at pH 10.3 comes from a pK_a of about 11.3. In the case of the binary complex with NAD^+, it is almost certain that, except for one ^{113}Cd NMR spectrum, which gave a signal close to the signal from the ternary complex with TFE^- (Bobsein & Myers, 1981), all earlier PAC and NMR spectra represent binary complexes with NADH and not NAD^+. We have, however, used an NAD^+ concentration 5-fold higher than that used in the earlier PAC and ^{113}Cd NMR work to enhance the NAD^+-bound fraction. This should be viewed in light of the 10-fold increase in NADH binding to the cadmium enzyme relative to the native enzyme and in light of the fact that it is virtually impossible to avoid traces of substrates that convert NAD^+ to NADH.

We can, for the first time, document the pH behavior of Cd_2Cd_2LADH, as is also evident from Figure 4. Our studies reveal a pK_a of 11.0 ± 0.2 for a change from the low-pH form to the high-pH form for $Cd_2(^{111m}Cd)Cd_2$LADH. Similarly, for the NAD^+ complex, an ionization with a pK_a of 9.6 ± 0.2 is found. The change in NQI for the free enzyme can be explained by the structural change, described earlier, caused by deprotonation of a metal-coordinated water. The change in NQI from low to high pH for the binary NAD^+ complex can also be explained by the deprotonation of metal-bound water. By assuming little change in the pK_a values from 25 to 1 °C (Kvassmann & Pettersson, 1979), the pK_a values found for the cadmium enzyme are in good agreement with the data for the zinc enzyme, since the higher ionic radius of Cd^{2+} is expected to increase the pK_a values in the former system. The pK_a values determined in this study for cadmium are based on the agreement between calculated and measured NQIs arising from ionization of a metal-coordinated water. Our data, therefore, support the view that the pK_a values found for the zinc enzyme likewise are due to the ionization of a metal-coordinated water (Kvassmann & Pettersson, 1979).

Comparison with Co_2Zn_2LADH Measurements. The pK_a values for Co_2Zn_2LADH of 9.4 (Dietrich & Zeppezauer, 1982) and for the Co_2Zn_2LADH−NAD^+ complex of 6.9 (Maret & Zeppezauer, 1986) are in good agreement with the values for the native enzyme and consistent with the increase of 2 pH units for the values determined for Cd_2Cd_2LADH. There is a pronounced correlation between PAC measurements and absorption spectroscopy: Whenever a band at 570 nm appears in the visible absorbance spectrum of Co^{2+}-substituted LADH, ω_0 is in the range 120−140 Mrad/s (free enzyme at high pH, with NAD^+ at high pH, with NAD^+ and Cl^- and with NAD^+ and TFE^-). The 570 nm band is also seen in rapid scanning stopped-flow experiments as an intermediate both in the conversion of alcohol to aldehyde and in the reverse reaction (Sartorius et al., 1987). This, together with information from ^{111m}Cd PAC spectroscopy, gives additional support for coordination of the substrate as an alcoholate ion, as was also suggested by Sartorius et al. (1987).

Variations in the Rigidity of the Metal Site of Cd_2Cd_2-LADH and in the Presence of NADH or NAD^+. For the free enzyme we find, except for the change as a function of pH between a low- and a high-pH form, only one coordination geometry for cadmium in the catalytic site. The large frequency distribution observed for the free enzyme corresponds to a flexible ligand sphere. This means that from one molecule to the next the coordination sphere is slightly different in the ligand−Cd−ligand angles. In contrast, the low value for the frequency distribution for the binary NAD^+ complex corresponds to a rigid ligand sphere. For the binary complex with NADH, each of the two NQIs have an even lower frequency distribution, corresponding to two well-defined coordination geometries, i.e., the ligands are fixed strongly at their respective positions. Therefore, it can be concluded that coenzyme binding to the enzyme produces a more rigid metal site.

Two Coordination Geometries in the Binary Complex with NADH. It is possible to crystallize the enzyme NADH complex in both the open and the closed conformations, depending on the conditions for crystallization (Cedergren-Zeppezauer, 1986). The presence of two conformations for the binary complex between the enzyme and NADH, observed via PAC spectroscopy, could be related to this. Since there is no change in the relative amounts of the two signals in the pH range, the equilibrium must be pH independent. The near 50% presence of each NQI (Table 2) could also arise from minor differences between the two subunits not observable by X-ray diffraction. It is also striking that upon the addition of DMSO to this complex only one sharp NQI is present.

ACKNOWLEDGMENT

We thank laboratory assistants Marianne Lund Jensen and Katja Brodersen, the cyclotron staff at the Niels Bohr Institute for Astronomy, Physics and Geophysics, Blegdamsvej, and the cyclotron staff at the University Hospital for their excellent assistance.

REFERENCES

Aeppli, H., Frauenfelder, H., & Walter, M. (1951) *Helv. Phys. Acta 24*, 335.

Al-Karadaghi, S., Cedergreen-Zeppezauer, E. S., Petratos, K., Hovmöller, S., Terry, H., & Wilson, K. S. (1994) *Acta Crystallogr. D 50*, 793−807.

Andersson, P., Kvassman, J., LIndström, A., Oldén, B., & Pettersson, G. (1981) *Eur. J. Biochem. 113*, 425−433.

Andersson, I., Bauer, R., & Demeter, I. (1982) *Inorg. Chim. Acta 67*, 53−59.

Bauer, R. (1985) *Q. Rev. Biophys. 18*, 1−64.

Bauer, R., Limkilde, P., & Johansen, J. T. (1976) *Biochemistry 15*, 334−342.

Bauer, R., Jensen, S. J., & Schmidt-Nielsen, B. (1988) *Hyperfine Interact. 39*, 203−234.

Bauer, R., Adolph, H. W., Andersson, I., Danielsen, E., Formicka, G., & Zeppezauer, M. (1991a) *Eur. Biophys. J. 20*, 215−221.

Bauer, R., Atke, A., Danielsen, E., Marcussen, J., Olsen, C. E., Rehfeld, J., Særmark, T., Schneider, D., & Zeppezauer, M. (1991b) *Appl. Radiat. Isotopes A 42*, 1015−1023.

Bauer, R., Bjerrum, M. J., Danielsen, E., & Kofod, P. (1991c) *Acta Chem. Scand. 45*, 593−603.

Bobsein, B. R., & Myers, R. J. (1981) *J. Biol. Chem. 256*, 5313−5316.

Bochmann, M., Bwembya, G. C., Grinter, R., Powell, A. K., Webb, K. J., Hursthouse, M. B., Malik, K. M. A., & Mazid, M. A. (1994) *Inorg. Chem. 33*, 2290−2297.

Butz, T., Saibene, S., Fraenzke, T., & Weber, M. (1989) *Nucl. Instrum. Methods Phys. Res. A284*, 417−421.

Cedergren-Zeppezauer, E. (1986) in *Zinc Enzymes* ed. I. (Bertini, I., Luchinat, C., Maret, W., & Zeppezauer, M., Eds.) pp 393−416, Birkhäuser, Boston.

Cedergren-Zeppezauer, E., Samama, J.-P., & Eklund, H. (1982) *Biochemistry 21*, 4895−4908.

Chandrasekhar, V., & Plapp, B. V. (1988) *Biochemistry 27*, 5082−5088.

Dalziel, K. (1957) *Acta Chem. Scand. 11*, 13−14.

Danielsen, E., Bauer, R., & Schneider, D. (1991) *Eur. Biophys. J. 20*, 193−201.

Dietrich, H., & Zeppezauer, M. (1982) *J. Inorg. Biochem. 17*, 227−235.

Dunn, M. F., Dietrich, H., Macgibbon, A. K. H., Koerber, S. C., & Zeppezauer, M. (1982) *Biochemistry 21*, 354−363.

Eklund, H., Nordström, B., Zeppezauer, E., Söderlund, G., Ohlsson, I., Bowie, T., Söderberg, B.-O., Tapia, O., Brändén, C. I., & Åkeson, Å. (1976) *J. Mol. Biol. 102*, 27−59.

Eklund, H., Samama, J.-P., Wallén, L., Brändén, C.-I., Åkeson, Å., & Jones, T. A. (1981) *J. Mol. Biol. 146*, 561−587.

Frauenfelder, H., & Steffen, R. M. (1965) in *Alpha-, Beta-, and Gamma ray spectroscopy* (Siegbahn, K., Ed.) Vol. 2, pp 997−1198, North-Holland, Amsterdam.

Kvassman, J., & Pettersson, G. (1979) *Eur. J. Biochem. 100*, 115−123.

Kvassman, J., & Pettersson, G. (1980) *Eur. J. Biochem. 103*, 557.

Kvassman, J., & Pettersson, G. (1987) *Eur. J. Biochem. 166*, 167−172.

Maret, W., & Zeppezauer, M. (1986) *Biochemistry 25*, 1584−1588.

Maret, W., Andersson, I., Dietrich, H., Schneider-Bernlohr, H., Einarsson, R., & Zeppezauer, M. (1979) *Eur. J. Biochem. 98*, 501−512.

Ramaswamy, R., Eklund, H., & Plapp, B. V. (1994) *Biochemistry 33*, 5230−5237.

Ryde, U. (1994) *Int. J. Quant. Chem. 52*, 1229−1243.

Sartorius, C., Gerber, M., Zeppezauer, M., & Dunn, M. F. (1987) *Biochemistry 26*, 871−882.

Skjeldal, L., Dahl, K. H., & McKinley-McKee, J. S. (1982) *FEBS Lett. 137*, 257−260.

Sytkowski, A. J., & Vallee, B. L. (1979) *Biochemistry 18*, 4095−4099.

BI9424555